

O. Barana, A. Murari, I. Coffey and JET EFDA contributors

Artificial Neural Networks for Real-Time Diagnostic of High-Z Impurities in Reactor-Relevant Plasmas

"This document is intended for publication in the open literature. It is made available on the understanding that it may not be further circulated and extracts or references may not be published prior to publication of the original when applicable, or without the consent of the Publications Officer, EFDA, Culham Science Centre, Abingdon, Oxon, OX14 3DB, UK."

"Enquiries about Copyright and reproduction should be addressed to the Publications Officer, EFDA, Culham Science Centre, Abingdon, Oxon, OX14 3DB, UK."

Artificial Neural Networks for Real-Time Diagnostic of High-Z Impurities in Reactor-Relevant Plasmas

O. Barana¹, A. Murari¹, I. Coffey² and JET EFDA contributors*

JET-EFDA, Culham Science Centre, OX14 3DB, Abingdon, UK

¹*Consorzio RFX – Associazione Euratom-ENEA sulla Fusione, Corso Stati Uniti 4, I-35127 Padova, Italy*
²*Queen’s University, Belfast, BT7 1NN, UK.*

** See annex of M.L. Watkins et al, “Overview of JET Results”,
(Proc. 21st IAEA Fusion Energy Conference, Chengdu, China (2006)).*

Preprint of Paper to be submitted for publication in Proceedings of the
IEEE International Symposium on Intelligent Signal Processing, Alcala de Henares- Madrid.
(3rd October 2007 - 5th October 2007)

ABSTRACT

The operation of JET with a new wall, made of beryllium in the main chamber and a tungsten divertor, will require additional care in handling plasma-wall interactions, since these new materials are certainly much less forgiving than the present ones. In particular, detecting tungsten will be extremely important not only for safety but also to understand the behaviour of high-Z impurities in reactor-relevant plasmas. In this paper Artificial Neural Networks are investigated to face the problem of real-time detection of high-Z impurities in plasma scenarios of ITER relevance. The data were collected with JET spectroscopy in a series of experiments, where laser blow-off was used to inject the various impurities. A wide range of plasma parameters was explored to cover the most important regions of the spectra. The good results obtained in recognizing the most important lines of the relevant materials prove that Artificial Neural Networks are strong candidates for real-time monitoring of the impurities both for protection purposes and for investigation of first-wall erosion.

I. INTRODUCTION

To support the design and operation of ITER, JET will be upgraded with a completely new wall, consisting of beryllium (Be) in the main chamber and tungsten (W) in the divertor [1]. This fully metallic wall will give the opportunity to test scenarios in an integrated way, taking into account the constraints and difficulties imposed by ITER materials. Monitoring the W content of the plasma will be crucial in two respects: a) to keep under control the status of the divertor and to monitor its erosion; b) to assess the behaviour of this impurity and its effects on the plasma performance. The safety issues linked to the wall integrity will require continuous surveying of various impurity lines and this will have to be done in an automatic way. W transport in the plasma will need first detection of the radiation emitted by the lower ionization stages to determine the influxes. The radiation emitted by higher ionization stages will provide the impurity content of the plasma core and detection will have to be optimized for the various temperature ranges of interest. To determine the impurity content, the W lines must also be properly discriminated from similar materials like hafnium (Hf), which has been considered as an implant in JET to study the erosion of plasma facing components. Therefore it is also important to detect timely their presence in JET plasmas. These problems linked with impurity monitoring will of course become even more difficult in ITER, whose discharges will last orders of magnitude longer than JET's, rendering manual solutions practically impossible. The complexity of this task of line identification for safety and scientific purposes motivated the investigation of the potential of Artificial Neural Networks (ANNs) in this field.

The development of ANNs was historically triggered by the interest in modelling the behaviour of the neurons in the human brain, but already one among the first publications in the field [2] dealt with important computational aspects. In the 1980s the back-propagation learning algorithm [3] acquired a lot of popularity. In those years it became clear not only that multilayer ANNs could model non-linear functions but also that a sound learning procedure was available.

Since the 1980s the development and progress in ANNs has constantly increased, so that the use

of ANNs has become common even in nuclear fusion applications. The ANN potential to implement non-linear transfer functions is very important in a domain characterized by complex and strong non-linear problems. In JET, for example, two ANNs have been trained and tested to provide the total radiated power and the divertor emission with an accuracy clearly better than the linear combination of chords [4], even though the implementation of the latter is usually rather basic. In the determination of the internal plasma inductance based on the Shafranov integrals, ANNs have also been successfully applied to determine this volume-dependent parameter [5], which is difficult to derive from the external magnetic measurements.

Up to now, in nuclear fusion, ANNs have probably found their most useful application in the real-time identification of several plasma parameters. In this context, ANNs offer clear advantages in terms of speed and generalization capabilities. This has suggested investigating their potential to detect high-Z impurities, in the framework of developing automatic survey techniques to reduce the need for human operators. The approach can also be of substantial help in scientific studies, because ANNs can, for example, provide a first screening of the data and identify the interesting lines, reducing the burden on the scientists, who normally have to devote a significant part of their time to this task.

Section 2 of this paper presents a brief summary of the requirements for spectroscopy in JET with the new all-metallic wall, which can certainly be considered a prototype of the ITER wall. Section 3 presents those architectural characteristics of ANNs that are particularly relevant to the applications described in this paper. The subject of Section 4 is the description of the experimental equipment used at JET to perform the blow-off of various impurities and to detect the relevant lines spectroscopically. Section 5 presents the results obtained by means of the ANNs developed for the detection of high-Z impurities relevant to JET and ITER walls, both in terms of bulk materials and erosion markers. Finally, the last section addresses the prospects of future and more advanced networks.

2. SPECTROSCOPY FOR WALL PROTECTION AND EROSION STUDIES IN PLASMAS OF REACTOR RELEVANCE

In the present generation of tokamaks, carbon is the most used material for the divertor, where most of the plasma-wall interaction takes place. The main advantages of this element are its high sublimation point of 3800 K and low Z . Instead of melting when reaching this temperature, it evaporates and then emits radiation in the plasma edge, reducing the peak loads on the wall. Despite these advantages, carbon is not a realistic candidate for a reactor, as it would be eroded too fast under reactor conditions [6]. Alternative wall materials, robust against sputtering by plasma particles, have therefore to be investigated. Moreover, it has been found in today's fusion devices, which operate with first walls of carbon fibre composites, that amorphous carbohydrate layers form inside the vacuum chamber during plasma operation. If similar layers formed in ITER, the co-deposited amount of tritium could hit the safety limit of 350g in less than 100 discharges, delaying further operation unacceptably. To overcome these problems, the present ITER design foresees a Be wall

with a W divertor, reducing the amount of graphite to a minimum, i.e. the tiles hit by the strike points. To prepare for ITER, at JET a new wall, with Be in the main chamber and a W divertor, is being designed. This upgrade will allow progressing the scenario development with the same mechanical boundary as ITER. This follows an extensive work performed at ASDEX Upgrade (AUG), the first large fusion experiment that implemented tungsten as a plasma facing material on a large scale, increasing the tungsten surface coverage from year to year [7].

However, notwithstanding the positive results obtained in AUG, plasma operation has to be conducted with great care in order to avoid large impurity influxes and excessive W concentrations in the plasma. From this experience, it has emerged very clearly that a basic pre-requisite, for operating a large fusion device with tungsten, is the ability to diagnose the impurity concentrations with the necessary accuracy, time and space resolution. Moreover, it is also extremely important to detect the increase in the W influxes and concentration very quickly, in order to allow the feedback systems to intervene in time, to guarantee safe operation of the machine and the successful execution of the scientific programme.

In addition to detecting impurities for wall protection, spectroscopy is also a fundamental tool to study erosion in general. JET has a strong research programme on Plasma-Wall Interactions (PWI). In this framework, the assessment of erosion and re-deposition of materials in the divertor region has always been considered an issue of high priority. Therefore in JET a dedicated program is focussing on investigating the possibility to deposit suitable materials (belonging to the transition metals and therefore with high atomic number Z) into the tiles and detect spectroscopically when the erosion has reached these implants [8]. Once in the main plasma these high Z transition metals emit characteristic lines, which have to be identified to assess how deeply the first wall has been eroded.

3. GENERAL DESCRIPTION OF THE ADOPTED NEURAL NETWORK

As mentioned in the introduction, ANNs are very useful to reduce the burden of human operators in the case of general surveying. As explained above, in future nuclear fusion experiments, it is very likely that the first wall erosion will be a major issue, requiring very close monitoring. To implement fast real-time control schemes, ANNs have the potential of being simple transfer functions, whose outputs can therefore be calculated on a sub-millisecond time scale. This could become a fundamental advantage when computational time is a crucial issue.

The general architecture of the adopted ANNs consists of a feedforward Multi-Layer Perceptron (MLP) with a single hidden layer, i.e. the ANNs are made of three layers: an input layer, a hidden layer and an output layer; each unit of a layer is connected, by means of weights connections, to every unit of the previous and/or the following layer [9]. A typical MLP scheme is shown in Fig.1, where the content of a perceptron (i.e. an ANN unit) is highlighted.

The relation that links the outputs y_k to the inputs x_i is given by

$$y_k = \hat{g} \left(\sum_{j=0}^m w_{kj} \cdot \hat{g}_j \left(\sum_{i=0}^d w_{ji} x_i \right) \right) \quad (1)$$

where g is a non-linear activation function (the hyperbolic tangent), \hat{g} a linear one and the w 's are the weights. It can be indeed demonstrated that at least in principle every continuous function can be reproduced by a feedforward ANN with a single hidden layer, for a finite range of the input values, and that, being g a non-linear activation function, an ANN has the ability of modelling in principle any arbitrary transfer function [9].

Since the ANNs are supervised, they need to be trained using the error back-propagation method. In particular, the ANNs for the identification of the marker materials use the Levenberg-Marquardt rule [9]. The error function is the following, which is proportional to the mean squared error:

$$E = \frac{1}{2} \sum_{k=1}^c (y_k - t_k)^2 \quad (2)$$

(where t_k is the k^{th} desired output). Though used in most applications, expression (2) does not represent the unique error function adopted in practice. In fact any error function whose derivative can be calculated at the output layer may be used instead, taking into account possible relations among the activation values of the output units.

4. JET LASER BLOW-OFF SYSTEMS AND SPECTROSCOPY

Heavy Z impurities were injected into JET plasmas using the laser ablation system [10,11]. A vacuum chamber located on one of the main JET horizontal ports contains the target holder. This consists of 15 separate glass slide targets ($49 \times 49 \text{ mm}^2$) coated with various materials. The laser itself is a single pulse ruby laser located outside the torus hall (694.3nm, 25ns pulse length, ~5-9 J). When the laser is fired onto the target it vaporizes a portion of the thin film coating (typically 3-5 μm thick), producing a burst of impurities which propagates towards the plasma. A 3mm diameter spot size produces a few 10^{18} atoms, although only a small fraction of this reaches the plasma giving an injected impurity concentration of the order of $10^{-4} n_e$ (where n_e is the electron density).

Many heavy Z species in the range $Z = 28$ to $Z = 83$ have been injected to study their spectroscopic signature and establish if they are distinguishable from each other using the available diagnostics on JET. Hf, tantalum (Ta), W, rhenium (Re), zirconium (Zr), molybdenum (Mo) and nickel (Ni) have all been injected using this method. The main spectroscopic region of interest on JET is in the soft X-ray to VUV (~1-100nm) [12]. An extreme-grazing-incidence Schwob-Frankel spectrometer [13] (SOXMOS, 1-340nm, 0.02nm resolution) and a grazing-incidence McPherson 251 spectrometer [14,15] (SPRED, 10-110nm, 0.3nm resolution) monitor the line emission spectra in this waveband. Both instruments have microchannel-plate/phosphor detectors, fibre-optically coupled to identical Princeton Instruments diode-array cameras. The maximum time resolution of both instruments is 11ms.

To further assess the effects of the injected impurities on the plasma the overall X-ray emission is measured using two soft X-ray cameras [16], and the radiated power P_{rad} is measured via the JET bolometer arrays [17]. Both of these instruments can give spatial and temporal data, allowing tomographic reconstruction of the evolution of the emission profiles. As the injections are often

parasitic to other experiments, the amount of impurity injected is usually set to provide the minimum useful signal, so as not to perturb the plasma unnecessarily. Normally a \hat{P}_{rad} of 1-2 MW is sufficient for this purpose.

5. ARTIFICIAL NEURAL NETWORK FOR REAL-TIME IDENTIFICATION AND CONTROL OF IMPURITIES

A dedicated ANN has been designed and trained by us to investigate the possibility of recognizing in real-time the spectroscopic fingerprint of the various marker materials once they are emitted from the main plasma. An example of the spectra in question is reported in Fig.2 for W, Hf and composite W/Hf targets. Another example is shown in Fig. 3 for Mo, Zr and Ni targets. The training set has been designed by first determining the best wavelength interval where the spectra differ most with respect to each other (found to be between 120Å and 200Å), and then excluding some spectra, in particular those belonging to the pre-ablation phase and the saturated ones (the level of saturation was of $4.2e^6$ counts/s). The threshold between the pre-ablation and the ablation spectra was set to be equal to $5e^5$ counts/s. This is identified by the black dashed lines in the Figures 2 and 3, which report, together with examples of ablation spectra (black solid lines), examples of pre-ablation spectra (grey solid lines). Finally, before feeding the ANN, the data were normalized with respect to the saturation level.

The architecture of the adopted feedforward Levenberg-Marquardt ANN consists of one input layer of 58 elements, one hidden layer of 10 elements and one output layer of 6 elements. The number of input units is the result of two operations: the restriction of the wavelength interval to 120Å–200Å and then the selection of one wavelength sample every three. The number of hidden units was chosen after several attempts as the least number of units that produce the desired output. Six is the number of output units and is equal to the number of examined materials (W, Hf, W/Hf, Mo, Zr and Ni). From this it is possible to understand that the ANN is used as a classifier; the input training and test sets consist of patterns whose associated outputs are arrays of zeros, except for the output element linked to the input pattern, whose value is one. Fig.4a shows a couple of input patterns (black line for W and grey line for Mo), while in Fig.4b the output patterns related to the inputs of Fig.4a are reported (circles for W and crosses for Mo). In this preliminary phase of the study, the data consisted of 136 patterns, three fourths of which were employed to train the ANN. Since the ANN is quite simple and the number of available input patterns is restricted, the time spent to train it was of a few seconds on a Pentium IV – 3.2GHz PC using Windows XP as operating system. The remaining fourth was used to test the network, which was able to classify successfully all the data patterns. It is worth noting that both the training set and the test set were chosen in order to have the same proportion of patterns related to the different elements.

6. FUTURE PROSPECTS

The use of ANNs in various fields of nuclear fusion, ranging from real-time and monitoring

applications to data analysis and modelling of non-linear transfer functions, can be considered generally very positive. The networks normally present better accuracy than the usual algorithmic approaches, require less computational time and can very often be upgraded with less manpower. These positive aspects have motivated the application study of a specific ANN for the real-time identification of spectral lines emitted by high-Z materials.

For the future we intend to include in the data set also spectra from other transition metals, like for example rhenium, to prove the versatility of the approach. Additional laser blow-off experiments are also being planned to increase the database and support the conclusions with better statistics.

As the complexity and the number of input patterns of the ANN increase, and to face the constraint related to the ANNs' extrapolation ability, a quality factor could be introduced in order to discard unpredictable outputs deriving from input patterns that lie outside the space defined by the training set. This quality factor can be a mean squared error computed on the outputs and would benefit from the fact of using, as output pattern, a gaussian function centred at the desired position instead of a pattern as in Fig.4b [18].

Once the ANN will have been intensively and successfully tested off-line, it will be ready to be checked on-line and, if no problems will be encountered, it will be possible to use it for the real time monitoring of the impurities.

The developed ANN could also be used in a more general framework of model-based feedback of injected impurities to achieve highly radiative plasmas. Indeed, in order to reduce the severity of PWIs in ITER, plasmas are planned to work at a radiated fraction of about 90%. Since in JET normally the radiation losses are of the order of 50% of the input power and they are going to decrease with the metallic wall, to study ITER-relevant scenarios, it will be important to increase radiation by injection of extrinsic low-Z impurities, like nitrogen. In order to optimize the efficiency of these impurities, also their density will have to be controlled in feedback, not only their radiation, as in present-day schemes. To this end ANNs of the type described in this paper could be used to quickly identify the necessary lines to be used by the models to quantify the impurity densities used for the feedback control of the radiation.

ACKNOWLEDGMENTS

This work was supported by the European Communities under the contract of Association EURATOM-UKAEA.

REFERENCES

- [1]. G.F. Matthews et al., "Overview of the ITER-like wall project", *Physica Scripta*, vol. **T128**, pp. 137-143, Mar. 2007.
- [2]. W.S. McCulloch and W. Pitts, "A logical calculus of the ideas immanent in nervous", *Bull. Math. Biophys.*, vol. **5**, pp. 115-133, 1943.
- [3]. A.E. Bryson and Y. Ho, *Applied Optimal Control*. New York: Blaisdell, 1969.

- [4]. O. Barana, A. Murari, P. Franz, L.C. Ingesson and G. Manduchi, "Neural Networks for Real Time Determination of Radiated Power in JET", *Rev. Sci. Instrum.*, vol. **73**, no. 5, pp. 2038-2043, May 2002.
- [5]. O. Barana, A. Murari, E. Joffrin, F. Sartori and contributors to the EFDA-JET Workprogramme, "Real-time Determination of Internal Inductance and Magnetic Axis Radial Position in JET", *Plasma Phys. Control. Fusion*, vol. **44**, no. 10, pp. 2271-2282, Oct. 2002.
- [6]. G. Janeschitz, ITER JCT and ITER HTs, "Plasma-wall interaction issues in ITER", *J. Nucl. Mater.*, vol. **290-293**, pp. 1-11, Mar. 2001.
- [7]. R. Neu, Tungsten as a Plasma Facing Material in Fusion Devices, Rep. IPP10/25, Max-Planck-Institut fuer Plasmaphysik, Garching, 2003.
- [8]. M.G. O'Mullane et al., "Diagnostic exploitation of complex heavy elements in tokamak plasmas", *Rev. Sci. Instrum.*, vol. **74**, no. 3, pp. 2080-2083, Mar. 2003.
- [9]. C.M. Bishop, *Neural Networks for Pattern Recognition*. Oxford: Oxford University Press, 1995.
- [10]. G. Magyar et al., JET Report No. JET-R(88)15, 1988.
- [11]. G. Magyar et al., JET Report No. JET-P(93)43, 1993.
- [12]. T. Puetterich, Investigation on Spectroscopy Diagnostics of High-Z Elements in Fusion Plasmas, Rep. IPP10/29, Max-Planck-Institut fuer Plasmaphysik, Garching, 2006.
- [13]. J.L. Schwob, A.W. Wouters, S. Suckewer and M. Finkenthal, "High-resolution Duomultichannel Soft X-ray Spectrometer for Tokamak Plasma Diagnostics", *Rev. Sci. Instrum.*, vol. **58**, no. 9, pp. 1601-1615, Sep. 1987.
- [14]. R.J. Fonck, A.T. Ramsey, and R.V. Yelle, "Multichannel grazing-incidence spectrometer for plasma impurity diagnosis: SPRED", *Appl. Opt.*, vol. 21, pp. 2115-2123, 1982.
- [15]. I.H. Coffey, R. Barnsley and JET EFDA Contributors, "First Tritium Operation of ITER-prototype VUV Spectroscopy on JET", *Rev. Sci. Instrum.*, vol. **75**, no. 10, pp. 3737-3739, Oct. 2004.
- [16]. B. Alper, S. Dillon, A.W. Edwards, R.D. Gill, R. Robins and D.J. Wilson, "The JET Soft X-ray diagnostic system", *Rev. Sci. Instrum.*, vol. **68**, no. 1, pp. 778-781, Jan. 1997.
- [17]. A. Huber et al., "Upgraded Bolometer System on JET for Improved Radiation Measurements", *Fusion Eng. Design*, in press.
- [18]. O. Barana et al., "A neural network approach for the detection of the locking position in RFX", *Fusion Eng. Design*, vol. **55**, pp. 9-20, May 2001.

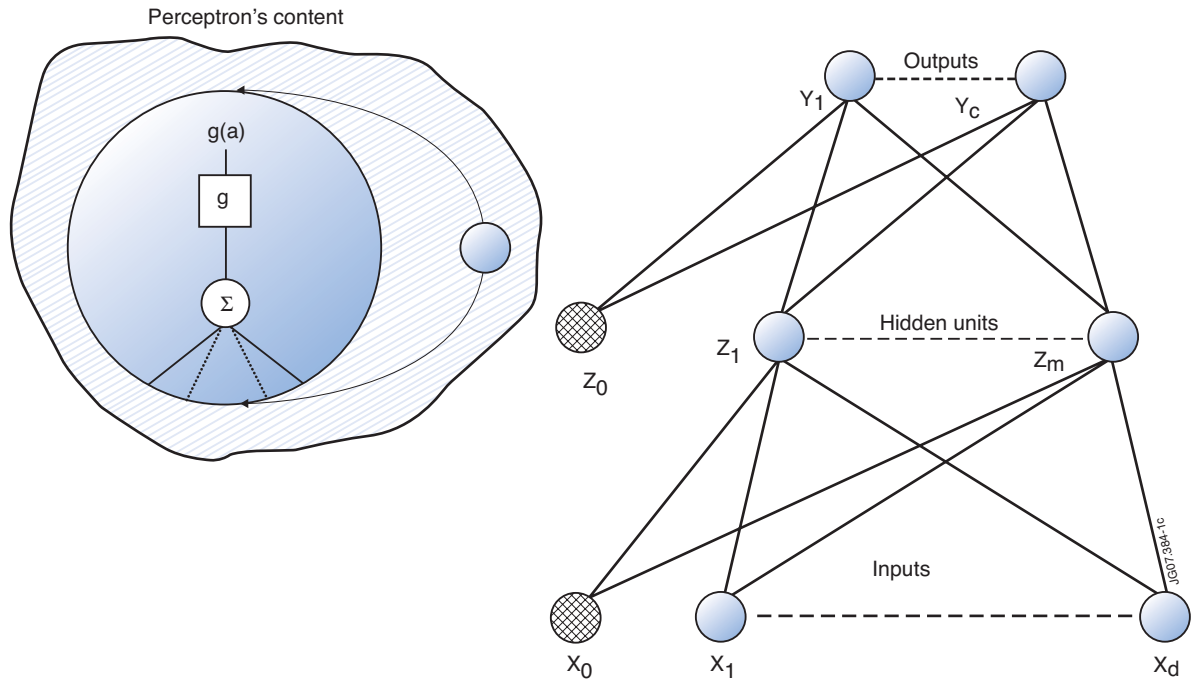


Figure 1: Pictorial view of a feedforward multi-layer perceptron. The content of a perceptron (i.e. an ANN unit) is highlighted.

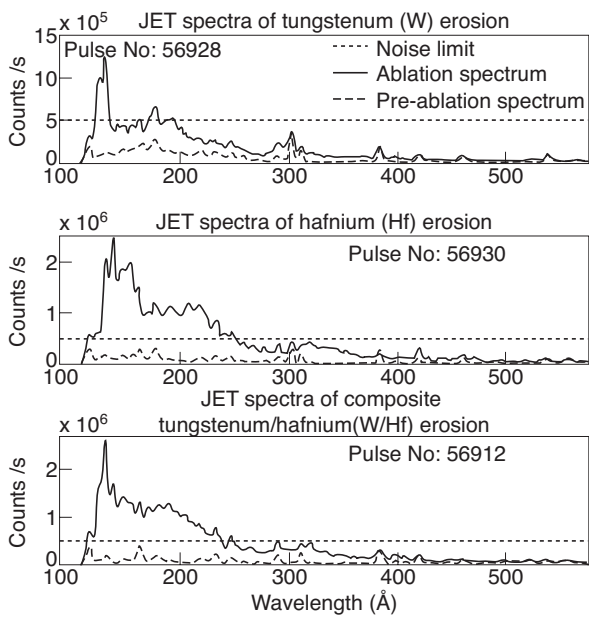


Figure 2: Example of JET spectra of tungsten (W), hafnium (Hf) and of composite W/Hf erosion markers. The solid black lines represent samples that were used to train the ANN. The solid grey lines represent pre-ablation samples that were excluded from the training sets. The black dashed lines identify the noise limit: a spectrum whose maximum is under this limit is not part of the training set.

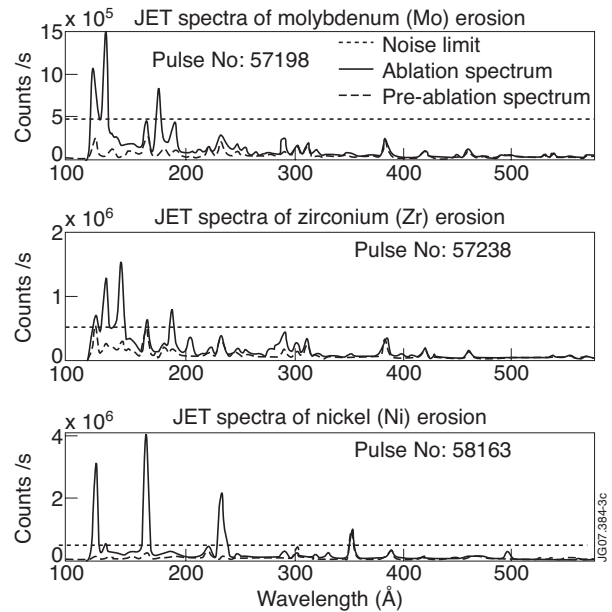


Figure 3: Example of JET spectra of molybdenum (Mo), zirconium (Zr) and nickel (Ni) erosion markers. The solid black lines represent samples that were used to train the ANN. The solid grey lines represent pre-ablation samples that were excluded from the training sets. The black dashed lines identify the noise limit: a spectrum whose maximum is under this limit is not part of the training set.

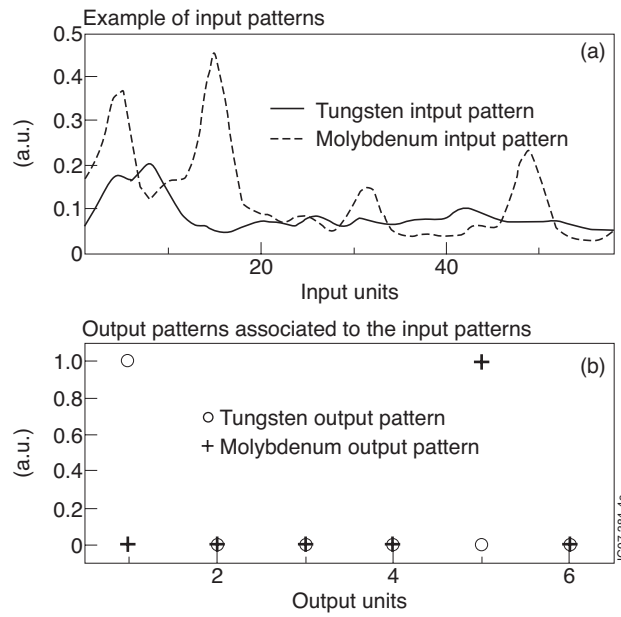


Figure 4: a) example of input patterns used to train the ANN: the black solid line is associated with a tungsten (W) sample, while the grey solid line is associated with Molybdenum (Mo); b) output patterns associated with the input patterns of Fig.4a: the circles are for W and the crosses for Mo.